RSC Advances

PAPER

View Article Online
View Journal | View Issue

Cite this: *RSC Adv.*, 2025, **15**, 8855

Box–Behnken optimized MPA-CdTe quantum dots as turn-off fluorescent probes for sensitive lurasidone determination in pharmaceutical, biological, and environmental matrices†

Razaz Abdulaziz Felemban,[ab] Maram H. Abduljabbar,[c] Reem M. Alnemari,[d] Rami M. Alzhrani,[d] Yusuf S. Althobaiti,[ce] Mohammed F. Aldawsari,[f] Ahmed Serag *[g] and Atiah H. Almalki*[eh]

A sensitive and selective fluorescence quenching method was developed for the determination of lurasidone using MPA-CdTe quantum dots as a "turn-off" fluorescent probe. The fluorescence intensity of the MPA-CdTe QDs was quenched upon the addition of lurasidone, with the quenching efficiency exhibiting a linear relationship with the lurasidone concentration in the range of 0.02–1.0 μg mL^{-1}. Stern–Volmer analysis revealed that the quenching mechanism was predominantly static in nature, and thermodynamic studies indicated that the interaction between lurasidone and MPA-CdTe QDs was exothermic and spontaneous in nature. Factors affecting the quenching process, including pH, MPA-CdTe QDs volume, and incubation time, were optimized using a Box–Behnken experimental design. A significant model was obtained with a coefficient of determination (R^2) of 0.9547, demonstrating the reliability of the optimization process. The analytical performance of the method was validated according to ICH guidelines, exhibiting good linearity and sensitivity with LOD of 5.90 ng mL^{-1} and LOQ of 17.70 ng mL^{-1}. The accuracy and precision of the method were assessed through recovery studies, showing satisfactory results with a mean recovery of 98.65 ± 0.733% and RSD% > 2%. The proposed method was successfully applied to the analysis of lurasidone in pharmaceutical dosage forms, spiked plasma, and environmental water samples, with good recoveries and precision. The greenness and analytical practicality of the method were evaluated using AGREE and BAGI tools, respectively, and the results showed that the proposed method is a greener and more practical alternative to previously reported analytical techniques for the determination of lurasidone. The present study demonstrates the potential of MPA-CdTe QDs as a sensitive and selective fluorescent probe for the determination of lurasidone in various matrices, with good analytical performance and environmental compatibility.

Received 21st January 2025
Accepted 17th March 2025

DOI: 10.1039/d5ra00519a

rsc.li/rsc-advances

1. Introduction

Fluorescent nanomaterials have gained significant attention in recent years due to their unique optical properties, high sensitivity, and potential for diverse analytical applications.[1,2] Various luminescent nanomaterials have been explored for analytical sensing, including carbon dots, metal–organic frameworks, and semiconductor quantum dots.[3–5] While carbon-based nanomaterials offer advantages in terms of biocompatibility and sustainable synthesis, and metal–organic frameworks provide unique structural versatility, they often face limitations in quantum yield, emission tunability, and detection sensitivity in complex matrices.[6,7] Among the range of fluorescent nanomaterials, CdTe semiconductor quantum dots have emerged as promising fluorescent probes, offering tunable emission wavelengths and excellent photostability.[8,9] When functionalized with 3-mercaptopropionic acid (MPA), these

[a]*Department of Basic Medical Sciences, College of Medicine, King Saud Bin Abdulaziz University for Health Sciences, Jeddah, Saudi Arabia*
[b]*King Abdullah International Medical Research Centre, Jeddah, Saudi Arabia*
[c]*Department of Pharmacology and Toxicology, College of Pharmacy, Taif University, P. O. Box 11099, Taif 21944, Saudi Arabia*
[d]*Department of Pharmaceutics and Industrial Pharmacy, College of Pharmacy, Taif University, P. O. Box 11099, Taif 21944, Saudi Arabia*
[e]*Addiction and Neuroscience Research Unit, Health Science Campus, Taif University, P. O. Box 11099, Taif 21944, Saudi Arabia. E-mail: ahalmalki@tu.edu.sa*
[f]*Department of Pharmaceutics, College of Pharmacy, Prince Sattam Bin Abdulaziz University, Al-kharj 11942, Saudi Arabia*
[g]*Pharmaceutical Analytical Chemistry Department, Faculty of Pharmacy, Al-Azhar University, Nasr City, 11751, Cairo, Egypt. E-mail: Ahmedserag777@hotmail.com*
[h]*Department of Pharmaceutical Chemistry, College of Pharmacy, Taif University, P. O. Box 11099, Taif 21944, Saudi Arabia*

† Electronic supplementary information (ESI) available. See DOI: https://doi.org/10.1039/d5ra00519a

quantum dots exhibit enhanced properties that make them particularly suitable for sensing applications.[10] The surface modification with MPA serves several key functions: it improves water solubility by introducing carboxyl groups, enhances biocompatibility for biological applications, and provides specific binding sites for target analytes.[11] Additionally, the surface passivation by MPA molecules significantly reduces surface defects, resulting in a substantial increase in quantum yield and photostability compared to bare CdTe QDs. The remarkable stability of MPA-CdTe QDs in aqueous media, combined with their strong fluorescence response to various analytes through different quenching mechanisms, has led to their widespread adoption in developing highly sensitive analytical methods.[12]

For example, a turn-off fluorescent sensor based on MPA-CdTe QDs has been reported for the detection of rifampicin and rifaximin through a quenching mechanism, demonstrating excellent sensitivity and selectivity.[13] Another study utilized MPA-CdTe QDs as a fluorescent probe for the sensitive determination of as "on–off–on" sensitive fluorescence probe to detect ascorbic acid *via* redox reaction.[14] The method is based on the selective quenching of the fluorescence of MPA-CdTe QDs by Fe^{3+} ions and the subsequent "turn-on" of the fluorescence upon the reduction of Fe^{3+} to Fe^{2+} by ascorbic acid. Building on these successful applications, the present study aims to investigate the potential of MPA-CdTe quantum dots as a highly sensitive fluorescent probe for the determination of lurasidone, an atypical antipsychotic drug used in the treatment of schizophrenia and bipolar disorder.

Lurasidone is a benzothiazole derivative with a unique pharmacological profile, characterized by high affinity for serotonin receptors, moderate affinity for dopamine and norepinephrine receptors, and low affinity for histamine and muscarinic receptors.[15–17] Due to its favorable receptor-binding profile, lurasidone has demonstrated efficacy in the treatment of various psychiatric disorders, including schizophrenia and bipolar depression, with a relatively low risk of adverse effects such as weight gain, sedation, and extrapyramidal symptoms.[18,19] However, the accurate determination of lurasidone in various matrices, including pharmaceutical formulations, biological samples, and environmental samples, remains a significant challenge due to the complex nature of the matrices and the low concentrations at which the drug is often present. Several analytical techniques have been employed for the determination of lurasidone, including high-performance liquid chromatography,[20,21] liquid chromatography-mass spectrometry,[22–25] and electrochemical methods.[26] However, these methods often suffer from limitations such as complex sample preparation, lengthy analysis times, and the requirement of specialized instrumentation. Fluorescent probes offer a promising alternative, as they can provide rapid, sensitive, and selective detection of lurasidone with minimal sample pretreatment. The only reported fluorescent-based method for the determination of lurasidone utilized erythrosine B as a fluorescent probe.[27] To the best of our knowledge, this work represents the first application of MPA-CdTe QDs for lurasidone determination, offering significant advantages in terms of photostability, quantum yield, and tunable emission wavelengths compared to conventional fluorophores, making them a more attractive choice for sensitive and selective analytical applications for this important atypical antipsychotic drug.[28]

Therefore, the present study aims to develop a highly sensitive and selective fluorescent sensing method for the determination of lurasidone using MPA-CdTe quantum dots as the fluorescent probe. The characterization of the MPA-CdTe QDs, including their size, morphology, and optical properties, will be carried out using techniques such as transmission electron microscopy, as well as UV-visible and spectrofluorimetric analyses. The mechanisms underlying the fluorescence quenching of MPA-CdTe QDs by lurasidone will be investigated using Stern–Volmer analysis and thermodynamic studies. The optimization of key experimental parameters will be performed using the Box–Behnken experimental design to achieve the best analytical performance. Furthermore, the proposed method will be subjected to comprehensive validation following the ICH guidelines to ensure its reliability, robustness, and suitability for real-world applications.

The validated method will then be applied to the analysis of lurasidone in pharmaceutical dosage forms, spiked plasma samples, and environmental water samples (river and tap water). Finally, the greenness and blueness of the developed method will be evaluated using the AGREE[29] and BAGI[30] tools, respectively, to assess its environmental impact and analytical practicality in comparison to the reported literature methods. This study aims to contribute to the development of a sensitive, selective, and environmentally friendly analytical method for the determination of lurasidone, which can have significant implications in pharmaceutical analysis, therapeutic drug monitoring, and environmental monitoring.

2. Experimental

2.1. Materials and reagents

Lurasidone hydrochloride (purity 99.85%), $NaBH_4$, Te powder, 3-MPA, and HPLC-grade solvents such as methanol, ethanol, and acetonitrile were purchased from Sigma-Aldrich (St. Louis, MO, USA). $CdCl_2 \cdot 2.5H_2O$, NaOH, and all other reagents were of analytical grade and obtained from Piochem Co., Cairo, Egypt. Distilled water was used throughout the experiments. Britton–Robinson buffer solutions (pH 5.0–10.0) were prepared according to standard procedures. Pharmaceutical formulation containing lurasidone (Elbaluran®, 20 mg) tablets was purchased from a local pharmacy, Cairo, Egypt.

2.2. Instrumentation

Jasco FP-6200 spectrofluorometer equipped with a xenon lamp as the excitation source was used for fluorescence measurements. The excitation and emission slit widths were set at 10 nm. Spectra Manager II software was used for data acquisition and processing. UV absorption spectra were recorded using a Shimadzu UV-1800 double beam spectrophotometer. Transmission electron microscopy (TEM) images were obtained using a JEM-2100 electron microscope operated at an acceleration

voltage of 200 kV. Fourier-transform infrared (FT-IR) spectra were recorded on a Nicolet iS5 FT-IR spectrometer in the wavenumber range of 4000–400 cm^{-1} using the KBr pellet technique. All pH measurements were carried out using a Jenway 3510 pH meter.

2.3. Synthesis and characterization of MPA-CdTe quantum dots

The MPA-CdTe quantum dots were synthesized following a previously reported procedure with minor modifications.[12] Briefly, Te powder (0.1 g) was mixed with $NaBH_4$ powder (0.07 g) in 4 mL of distilled water under vigorous stirring, and the mixture was deoxygenated with nitrogen gas in an ice bath for 6 hours to yield freshly prepared NaHTe. Two mL of the resulting NaHTe aqueous solution was transferred to another flask containing $CdCl_2$ (0.1 g) and 200 μL of MPA in 60 mL of deoxygenated water. The solution was adjusted to pH 9 using 1 M NaOH and refluxed at 100 °C for 10 hours to obtain the MPA-capped CdTe QDs. The QDs were purified by repeated precipitation with acetone and centrifugation. A stock solution of the MPA-CdTe QDs was prepared in distilled water by dissolving the MPA-CdTe QDs at a concentration of 2 mg mL^{-1}. The synthesized MPA-CdTe QDs were characterized by TEM, FT-IR, UV-visible spectroscopy, photoluminescence spectroscopy to determine their size, morphology, structure and optical properties.

2.4. Construction of the fluorescent sensor

Optimization of the sensing conditions was first carried out to achieve the highest sensitivity. Different parameters, including MPA-CdTe QDs concentration, pH of the medium, and incubation time, were optimized using the Box–Behnken experimental design. Initial screening experiments were performed to determine the suitable range for each parameter. The pH was studied in the range of 5.0–10.0 using Britton–Robinson buffer, the MPA-CdTe QDs volume varied from 0.5 to 1.5 mL and the incubation time was optimized between 1 and 5 minutes. With 5 central points, a total of 17 experimental runs were conducted (Table S1†). A quadratic model was fitted to the data, and the optimal conditions were determined by analyzing the response using Design-Expert software.

The optimized fluorescent sensing protocol was as follows: to a 10 mL volumetric flask, different aliquots of the lurasidone working standard solution (2 μg mL^{-1}) were added, followed by 1.25 mL of the MPA-CdTe QDs stock solution and 1 mL of Britton–Robinson buffer (pH 7.8). The solution was left to stand for 2.7 minutes at room temperature and the volume was made up to the mark with distilled water. The fluorescence intensity was measured at the excitation and emission wavelengths of 350 nm and 575 nm, respectively (F). A blank solution containing all the components except lurasidone was prepared and measured under the same conditions (F_0).

2.5. Method validation

The developed fluorescent method was validated according to the ICH guidelines in terms of linearity, sensitivity, accuracy, precision, selectivity, and robustness. Linearity was evaluated by constructing calibration curves using six standard solutions of lurasidone in the range of 0.02–1.0 μg mL^{-1}. The linearity was assessed by the correlation coefficient (r^2) and the linear regression equation. The limit of detection and limit of quantification were calculated based on the standard deviation of the residuals and the slope of the calibration curve according to the following equations:

$$\mathrm{LOD} = 3.3 \times \sigma/S$$

$$\mathrm{LOQ} = 10 \times \sigma/S$$

where σ is the standard deviation of the residuals and S is the slope of the calibration curve.

The accuracy of the method was determined by recovery studies at three different concentration levels (0.05, 0.5, and 0.8 μg mL^{-1}) and the results were expressed as the percentage of the recovered amount compared to the spiked amount. The precision of the method was evaluated in terms of repeatability and intermediate precision and expressed as the relative standard deviation (RSD%). The selectivity of the method was investigated by analyzing common excipients and potential interferent ions such as Na^+, K^+, Ca^{2+}, Cd^{2+}, Ni^{3+}, Cl^-, PO_4^{3-}, and SO_4^{2-} at 10-fold excess over the analyte concentration and the quenching effect was compared to the analyte alone. The robustness of the method was evaluated by intentionally varying parameters such as the pH and MPA-CdTe QDs volume and the effect on the analytical response was observed followed by recovery studies.

2.6. Application to real samples

Ten lurasidone tablets were accurately weighed and finely powdered. An appropriate amount of the powder equivalent to 10 mg of lurasidone was dissolved in 80 mL ethanol, sonicated for 10 minutes, filtered, and made up to 100 mL with ethanol. A working solution was prepared by diluting this stock solution with ethanol to obtain a final concentration labeled to contain 2.0 μg mL^{-1} of lurasidone. The optimized fluorescent sensing protocol was applied to determine the lurasidone content in the tablet samples within the established linear range.

For the analysis of spiked plasma, 10 mL of fresh pooled human plasma was spiked with lurasidone at four concentration levels to obtain final concentrations of 0.02, 0.05, 0.1, and 0.5 μg mL^{-1}. The plasma samples were processed by protein precipitation with 3 mL acetonitrile, centrifuged at 12 000 rpm for 15 minutes, and the supernatant was collected. The resulting clear solution was evaporated to dryness under a gentle stream of nitrogen, reconstituted with 2 mL of ethanol, then transferred to a 10 mL volumetric flask, and the fluorescent sensing protocol was applied. The developed fluorescent sensor was also applied to determine lurasidone in spiked environmental water samples, including tap water and river water. To a 10 mL volumetric flask, 2 mL of the water sample was spiked with lurasidone at different concentration levels, and the optimized fluorescent sensing protocol was followed without any further pre-treatment. Recovery studies were performed to

evaluate the accuracy of the method in the analysis of these real samples. In addition, RSD% values were calculated to assess the precision of the measurements.

3. Results and discussion

3.1. Characterization of MPA-CdTe QDs

The synthesized MPA-capped CdTe quantum dots were thoroughly characterized using complementary analytical techniques to confirm their structural and optical properties. TEM analysis revealed well-dispersed, spherical nanoparticles with an average diameter of approximately 3.12 nm (Fig. 1A). The TEM micrograph shows clearly defined quantum dots with good monodispersity and minimal aggregation, indicating successful synthesis.

FTIR spectroscopy was employed to confirm the successful surface modification of CdTe QDs with MPA (Fig. 1B). The FTIR spectrum of free MPA exhibited characteristic peaks at approximately 3600–3400 cm^{-1} (O–H stretching), 2900–2800 cm^{-1} (C–H stretching), and prominent bands in the 1700–1600 cm^{-1} region (C═O stretching of COOH). In the spectrum of MPA-CdTe QDs, several significant changes were observed. The characteristic peaks in the 2400–2000 cm^{-1} region showed increased intensity in the MPA-CdTe QDs compared to free MPA, indicating structural modifications during the capping process. Additionally, notable differences in the fingerprint region (1600–400 cm^{-1}) confirm the successful binding of MPA to the QD surface. The spectral pattern in this region displays altered peak intensities and slight shifts, particularly around 1400–1200 cm^{-1}, which can be attributed to the interactions between the carboxyl groups of MPA and the Cd atoms on the QD surface. The spectral differences between free MPA and MPA-CdTe QDs provide strong evidence for the successful capping of CdTe QDs with MPA, essential for the subsequent fluorescence-based detection of lurasidone.

Optical characterization revealed distinct features indicative of high-quality MPA-CdTe QDs. The UV-vis absorption spectrum exhibited a pronounced absorption peak at 544 nm, corresponding to the first excitonic transition, which confirms the narrow size distribution and quantum confinement effect (Fig. 1C). The fluorescence emission spectra showed a strong, symmetric emission peak centered at 575 nm, characteristic of the intrinsic bandgap luminescence of the MPA-CdTe QDs. Upon varying the excitation wavelengths from 350 nm to 380 nm, the emission intensity decreased slightly without any observable shift in the peak position, further confirming that the emission originates from the bandgap rather than surface trap states (Fig. 1D). These results collectively demonstrate the successful synthesis of high-quality MPA-CdTe QDs with superior photophysical properties suitable for further applications. The quantum yield of the MPA-CdTe QDs was determined to be 29.7% using quinine sulfate as the reference standard, indicating their potential as efficient fluorescent probes.

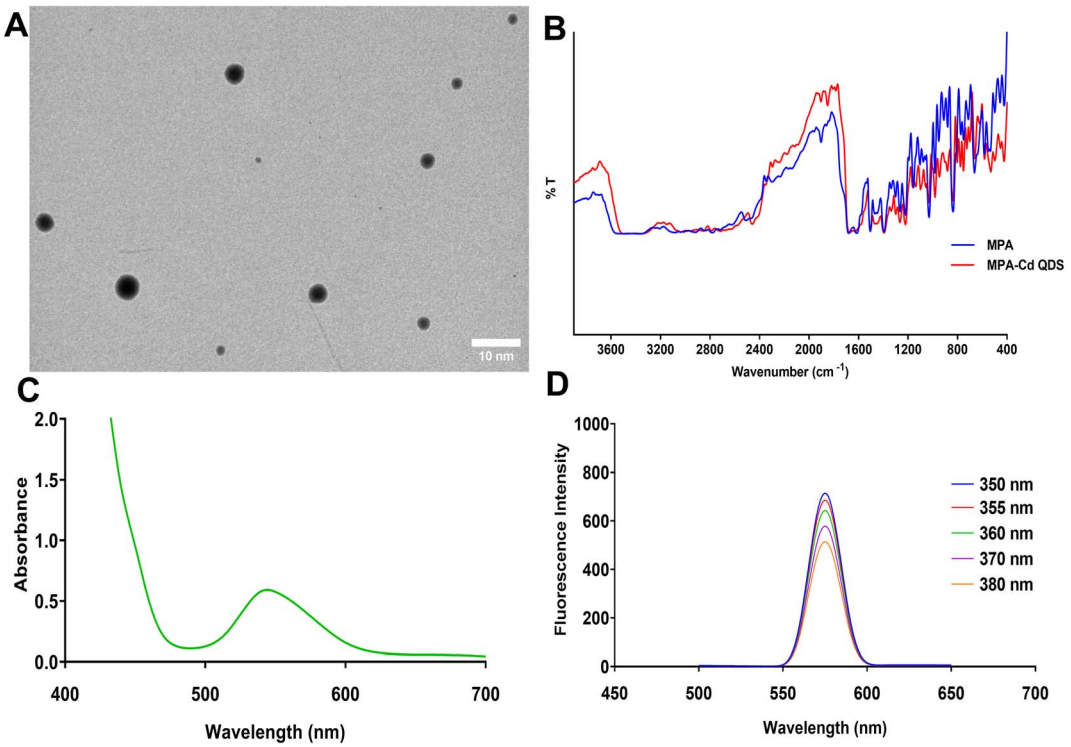

Fig. 1 Physical and optical characterization of MPA-CdTe quantum dots. (A) Transmission electron microscopy (TEM) image of well-dispersed, spherical MPA-CdTe QDs with scale bar = 10 nm. (B) FTIR spectra comparing free MPA (blue line) and MPA-CdTe QDs (red line), demonstrating successful surface functionalization. (C) UV-visible absorption spectrum displaying characteristic first excitonic peak at 544 nm. (D) Fluorescence emission spectra at different excitation wavelengths (350–380 nm) showing consistent emission peak at 575 nm.

3.2. Sensing mechanism of lurasidone detection

The fluorescence properties of the MPA-CdTe QDs were investigated in the presence of lurasidone. Upon addition of increasing concentrations of lurasidone to the MPA-CdTe QDs solution, a progressive and significant quenching of the fluorescence intensity was observed (Fig. 2A). Such quenching behavior suggests a strong interaction between the lurasidone and the MPA-CdTe QDs, enabling their use as a fluorescent "turn-off" sensor for the determination of lurasidone. To elucidate the quenching mechanism, Stern–Volmer analysis was performed by plotting the ratio of the fluorescence intensity of the MPA-CdTe QDs in the absence (F_0) and presence (F) of lurasidone as a function of the lurasidone concentration at different temperatures (298 K, 303 K, and 308 K). The Stern–Volmer plots exhibited good linearity, indicating a single quenching mechanism, either static or dynamic (Fig. 2B). The Stern–Volmer quenching constant was determined from the slope of the linear plot according to:

$$\frac{F_0}{F} = 1 + K_{SV}[Q]$$

where F_0 and F are the fluorescence intensities of the MPA-CdTe QDs in the absence and presence of lurasidone, respectively, and K_{SV} is the Stern–Volmer quenching constant.

The calculated K_{SV} values at 298 K, 308 K, and 318 K were 8.77×10^5, 7.52×10^5, and 6.51×10^5 M^{-1}, respectively (Table 1). The decrease in the K_{SV} values with increasing temperature suggests that the quenching mechanism is primarily static in nature, arising from the formation of a ground-state complex between lurasidone and the MPA-CdTe QDs. Furthermore, the diffusion-controlled dynamic quenching constant (K_q) was calculated using the equation:

$$K_{SV} = K_q \tau_0$$

where τ_0 is the fluorescence lifetime of the MPA-CdTe QDs in the absence of lurasidone, estimated to be 9.6 ns. The K_q values were on the order of 10^{14} L mol^{-1} s^{-1}, which is much higher than the maximum diffusion-controlled quenching rate constant (2×10^{10} L mol^{-1} s^{-1}), further confirming that the quenching is predominantly static in nature. The modified Stern–Volmer analysis (Fig. 2C) was performed to determine the association constant (K_a) according to:

$$\frac{F_0}{F_0 - F} = \frac{1}{[Q]K_a} + \frac{1}{K_a}$$

It was found that the association constant at 298 K was 1.54×10^6 M^{-1}, which indicates a strong binding affinity between lurasidone and the MPA-CdTe QDs. Upon increasing the temperature, the K_a decreased, suggesting that the binding process is exothermic in nature (Table 1).

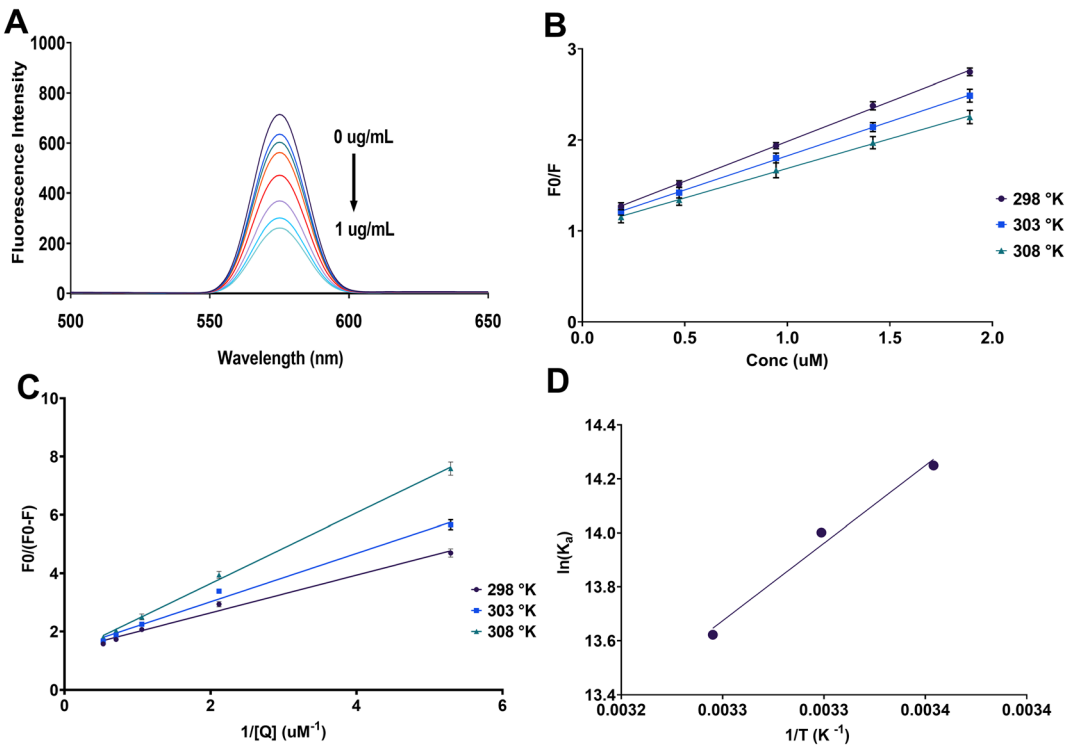

Fig. 2 Fluorescence quenching analysis of MPA-CdTe QDs with lurasidone. (A) Fluorescence emission spectra of MPA-CdTe QDs showing progressive quenching with increasing lurasidone concentration (0–1 μg mL^{-1}). (B) Stern–Volmer plots (F_0/F *vs.* lurasidone concentration) at different temperatures (298 K, 303 K, and 308 K) showing linear relationships indicative of a single quenching mechanism. Error bars represent standard deviation of triplicate measurements ($n = 3$). (C) Modified Stern–Volmer plots ($F_0/(F_0 - F)$ *vs.* 1/[Q]) at different temperatures for determination of the association constant (K_a). Error bars represent standard deviation of triplicate measurements ($n = 3$). (D) van't Hoff plot ($\ln(K_a)$ *vs.* $1/T$) for the determination of thermodynamic parameters of the binding interaction between lurasidone and MPA-CdTe QDs.

Table 1 Temperature-dependent binding parameters and thermodynamic data characterizing the interaction between MPA-CdTe QDs and lurasidone

Temperature (K)	K_{sv} (10^5 M^{-1})	K_a (10^6 M^{-1})	ΔG (kJ mol^{-1})	ΔH (kJ mol^{-1})	ΔS (J mol^{-1} K^{-1})
298	8.77	1.54	−35.32	−47.90	−42.19
303	7.52	1.20	−35.29		
308	6.51	0.82	−34.90		

The previous finding was corporate by the thermodynamic parameters calculated from the temperature-dependent fluorescence quenching data using the van't Hoff plot (Fig. 2D). The negative values of ΔG at all the studied temperatures indicate a spontaneous binding process (Table 1). The negative value of ΔH (−47.90 kJ mol^{-1}) suggests that the binding is exothermic, corroborating the static quenching mechanism. Moreover, the negative value of ΔS (−42.19 J mol^{-1} K^{-1}) indicates that the binding is accompanied by a decrease in the entropy of the system, which could be attributed to the formation of the ground-state complex with a more ordered configuration. It is worth mentioning that the inner filter effect caused by the absorption of lurasidone was negligible as no significant absorption was observed in the excitation or emission wavelength regions.

Based on these findings, the sensing mechanism primarily involves the formation of a ground-state complex between lurasidone and MPA-CdTe QDs through multiple interaction sites. The carboxyl groups of MPA on the QD surface can interact with the multiple nitrogen atoms in lurasidone's structure (piperazine ring, benzothiazole moiety, and imide group) through electrostatic attractions. Additionally, hydrogen bonding can occur between the surface –OH groups of MPA-CdTe QDs and the carbonyl groups of the imide moiety in lurasidone. The benzothiazole ring system may also participate in π–electron interactions with the QD surface. This multi-point binding leads to efficient fluorescence quenching through electron transfer from the excited state of QDs to the electron-deficient regions of lurasidone.

3.3. Optimization of fluorescence quenching conditions

The fluorescence quenching of MPA-CdTe QDs by lurasidone was further investigated by optimizing the critical parameters affecting the sensitivity of the sensing system, including pH, MPA-CdTe QDs volume, and incubation time. The effects of these parameters were studied using a Box–Behnken design, and the results were analyzed by fitting a response surface quadratic model using multiple linear regression. Backward elimination was applied to refine the model and ANOVA analysis showed that the proposed reduced model was significant ($p < 0.0001$) with a lack of fit that was not significant ($p = 0.3406$), indicating a good fit of the experimental data (Table S2†). Additionally, two factors (pH and MPA-CdTe QDs volume) were found to have a significant effect on the fluorescence quenching efficiency, while the incubation time had no significant impact. It is worth noting that a quadratic effect was observed for these two significant factors suggesting the existence of an optimal value within the experimental domain (Table S2†). The final equation in terms of coded factors was:

$$R = 2.21947 + 0.199625A + 0.234733B - 0.447641A^2 - 0.194011B^2$$

where R is the fluorescence quenching response (F_0/F), A is the pH, and B is the MPA-CdTe QDs volume. The positive coefficients for the linear terms indicate that fluorescence quenching increases as the pH and MPA-CdTe QDs volume increase, while the negative coefficients for the quadratic terms suggest the existence of an optimum level for these factors. This comes in line with the observation that the fluorescence quenching response increased with increasing pH, reaching a maximum around pH 7.8, and then decreased at higher pH values (Fig. 3A). Also, the quenching efficiency increased with increasing MPA-CdTe QDs volume, attaining a maximum around 1.25 mL, after which it slightly declined (Fig. 3B). The incubation time was found to have a negligible effect on the fluorescence quenching over the tested range of 1–5 min, suggesting that the binding equilibrium between lurasidone and MPA-CdTe QDs is rapidly achieved (Fig. 3C). The 3D-response surface plot of pH and MPA-CdTe QDs clearly demonstrates the optimal region to maximize the fluorescence quenching response (Fig. 3D). It should be noted that pH below 5 and above 10 were avoided due to potential interference with the luminescence properties of the QDs. As the media become more acidic, aggregation and precipitation of the MPA-CdTe QDs can occur, while at high pH values, lurasidone becomes in its deprotonated form, reducing its ability to interact with the MPA-CdTe QDs. The potential interaction effects between pH and MPA-CdTe QDs volume were also investigated during the model development phase. The interaction term was found to be statistically insignificant ($p > 0.05$) during the backward elimination process and was therefore excluded from the final reduced model. This absence of significant interaction is visually demonstrated in (Fig. S1†), where the parallel nature of the response curves at different factor levels indicates that the effect of pH on fluorescence quenching remains consistent across different QDs volumes. The lack of significant interaction between these factors suggests that their effects on the fluorescence quenching response are independent of each other, which contributes to method optimization simplification and analytical procedure robustness enhancement.

Validation of the developed model was conducted by observing several criteria and diagnostic plots. The variance was explained with an R^2 of 0.9547, indicating an excellent fit of the

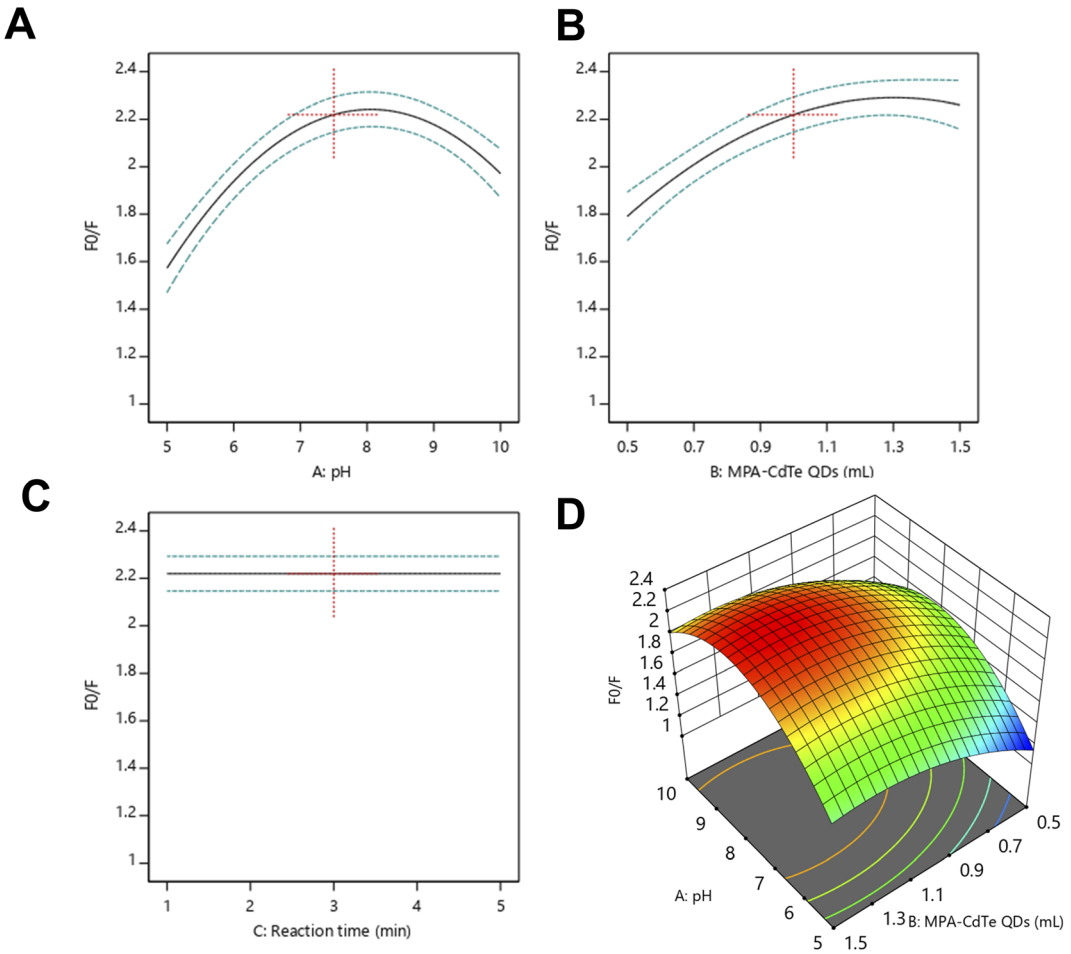

Fig. 3 Optimization of experimental parameters affecting the fluorescence quenching response of MPA-CdTe QDs by lurasidone. (A) Effect of pH on the fluorescence quenching response (F_0/F) showing optimal quenching at pH 7.8. (B) Influence of MPA-CdTe QDs volume on quenching efficiency with maximum response at approximately 1.25 mL. (C) Effect of reaction time on the quenching response showing rapid equilibrium achievement within 1–5 minutes. (D) Three-dimensional response surface plot illustrating the combined effects of pH and MPA-CdTe QDs volume on the fluorescence quenching response.

experimental data. The adjusted R^2 and predicted R^2 were 0.9396 and 0.8967, respectively, with an insignificant lack of fit, confirming the validity of the model. The actual *vs.* predicted plot showed that the developed model can accurately predict the experimental responses (Fig. S2A†), and the predicted *vs.* the residual plot did not reveal any obvious patterns, indicating the absence of bias in the model (Fig. S2B†). Examination of the residual and leverage *vs.* run order plots did not reveal any outliers or influential data points indicating the absence of experimental errors (Fig. S3†).

Numerical and graphical optimization was performed to determine the optimal conditions for maximum fluorescence quenching. The criteria were set to maximize the fluorescence quenching response while maintaining pH and MPA-CdTe QDs volume within the experimental range. Desirability function analysis identified optimal conditions at pH 7.8 and 1.25 mL of MPA-CdTe QDs, yielding a maximum predicted fluorescence quenching response (F_0/F) of 2.30 (Fig. S4A†). The overlay plot (Fig. S4B†) visualizes these results, with the yellow region indicating the optimal zone where pH, QD volume and the fluorescence quenching response constraints are simultaneously satisfied. The optimal pH of 7.8 represents a critical balance point in the system – at pH below 5, MPA-CdTe QDs risk aggregation and precipitation, while at pH above 10, lurasidone becomes deprotonated, diminishing its interaction with the QDs as previously discussed. Similarly, the optimal MPA-CdTe QDs volume of 1.25 mL achieves a balance between providing sufficient sensing sites and avoiding self-quenching effects that could occur at higher concentrations. The overlay plot effectively illustrates this optimal region, serving as a practical guide for selecting operational parameters that maximize quenching efficiency while maintaining system stability. This optimization approach not only maximizes the analytical signal but also ensures robust performance by operating within a stable pH range that aids in reliable measurements.

3.4. Validation of the analytical method

The analytical method was validated according to the ICH guidelines in terms of linearity, sensitivity, accuracy, precision, robustness, and selectivity.

Linearity was evaluated by constructing a calibration curve using standard solutions of lurasidone in the concentration range of 0.02–1.0 μg mL^{-1}. The linear regression equation was $y = 1.1011x + 1.6665$ with a correlation coefficient (r^2) of 0.9995, indicating excellent linearity within the tested range (Table 2). The limit of detection and limit of quantitation were found to be 5.90 ng mL^{-1} and 17.70 ng mL^{-1}, respectively, demonstrating high sensitivity of the proposed method (Table 2). Accuracy was assessed by analyzing lurasidone at three different concentration levels (0.05, 0.5, and 0.8 μg mL^{-1}) in triplicate, and the mean recovery was 98.65 ± 0.733% indicative of excellent accuracy. The intra-day and inter-day precision, expressed as relative standard deviation, were less than 2% for both repeatability and intermediate precision, confirming the high precision of the method (Table 2).

Robustness was evaluated by deliberately varying the critical method parameters such as pH (7.6–8.0) and MPA-CdTe QDs volume (1.2–1.3 mL) within the optimal ranges determined by the DoE. The percentage recovery remained within 98–102%, indicating the robustness of the proposed method (Table 2). Selectivity was evaluated by analyzing samples containing potential interferents at 10-fold higher concentrations than lurasidone. Common pharmaceutical excipients (lactose, starch, magnesium stearate, and talc) and ionic species (Na^+, K^+, Ca^{2+}, Cd^{2+}, Ni^{3+}, Cl^-, PO_4^{3-}, SO_4^{2-}, Fe^{3+}, Cu^{2+}, and Hg^{2+}) were tested (Fig. 4). While most species showed negligible interference (<5% signal change), Fe^{3+}, Cu^{2+}, and Hg^{2+} exhibited moderate interference (15%, 12%, and 8% signal change respectively). This interference was successfully mitigated by adding EDTA (0.1 mM) for Fe^{3+} and Cu^{2+}, and thiourea (0.1 mM) for Hg^{2+}, reducing the interference to <5% in all cases (Fig. 4). Biological components such as glucose, uric acid, and various amino acids including glycine, alanine, and glutamic acid also showed minimal interference (<5%), demonstrating the method's suitability for plasma analysis (Fig. 4). Under these optimized conditions, the method demonstrated excellent selectivity for lurasidone determination in pharmaceutical, biological, and environmental matrices.

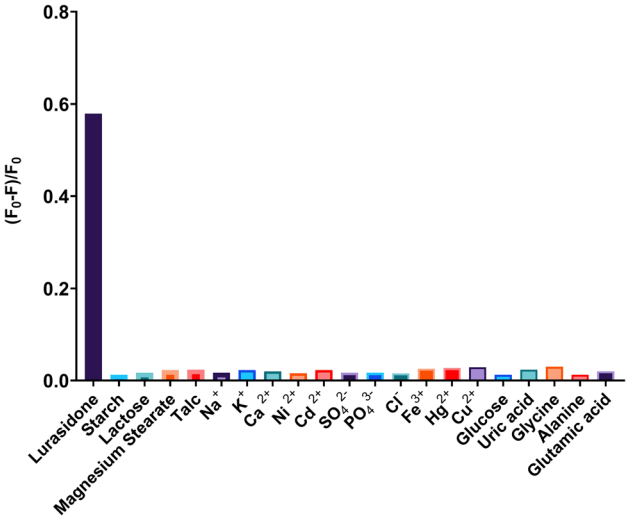

Fig. 4 Evaluation of selectivity of the developed MPA-CdTe QDs-based fluorescence quenching method showing the fluorescence quenching ratio $(F_0 - F)/F_0$ for lurasidone compared to common pharmaceutical excipients (starch, lactose, magnesium stearate, talc), ionic species (Na^+, K^+, Ca^{2+}, Ni^{2+}, Cd^{2+}, SO_4^{2-}, PO_4^{3-}, Cl^-, Fe^{3+}, Hg^{2+}, Cu^{2+}), and biological interferents (glucose, uric acid, glycine, alanine, glutamic acid). The significantly higher quenching ratio observed for lurasidone demonstrates the high selectivity of the method for the target analyte in the presence of potential interferents commonly found in pharmaceutical, environmental and biological matrices.

Table 2 Summary of analytical method validation parameters for the fluorescence-based determination of lurasidone using MPA-CdTe quantum dots

Parameters		Lurasidone
Excitation wavelength (nm)		350
Emission wavelength (nm)		575
Linearity range (μg mL^{-1})		0.02–1.00
Slope		1.6665
Intercept		1.1011
Correlation coefficient (r^2)		0.9995
LOD (ng mL^{-1})		5.90
LOQ (ng mL^{-1})		17.70
Accuracy (% R)[a]		98.65 ± 0.733
Repeatability precision (% RSD)[b]		0.743
Intermediate precision (% RSD)[c]		1.517
Robustness (% R)	Buffer (pH)	99.16 ± 1.06
	MPA-CdTe QDs (mL)	101.31 ± 1.257

[a] Average of 9 determinations (3 concentrations repeated 3 times). [b] % RSD of 9 determinations (3 concentrations repeated 3 times) measured on the same day. [c] % RSD of 9 determinations (3 concentrations repeated 3 times) measured in the three consecutive days.

3.5. Application of the developed method

The developed MPA-CdTe QDs based fluorescence quenching method was successfully applied for the determination of lurasidone in pharmaceutical dosage forms, spiked plasma, and environmental water samples (river and tap water). The average recovery of lurasidone in pharmaceutical formulations was 100.49 ± 1.040%, demonstrating the applicability of the method for routine quality control analysis (Table S3†). Furthermore, statistical comparison of the results obtained by the proposed method with those from a reported HPLC method[21] showed no significant difference as evident from the Student's t-test and F-test with $t = 0.330$ and $F = 1.099$, which are lower than the tabulated values (2.306 and 6.338 at $P = 0.05$), confirming the accuracy and precision of the proposed method (Table S3†). Interval hypothesis testing of the results showed that the bias values ($\theta_L = -1.270$ and $\theta_U = 1.695$) were within the acceptable ±2% range, confirming the reliability of the proposed method.

The developed method was also applied to the analysis of lurasidone in spiked plasma and environmental water samples (Table 3). The mean recovery of lurasidone in spiked plasma samples ranged from 95.53 to 103.85%, with RSD% ≤ 3.321%, demonstrating the ability of the method to accurately quantify lurasidone in complex biological matrices. The analysis of lurasidone in spiked river water samples resulted in recovery rates

Table 3 Recovery studies for lurasidone determination in spiked plasma and environmental water samples (river and tap water) using the MPA-CdTe QDs fluorescence quenching method

Samples	Spiked (μg mL^{-1})	Found (μg mL^{-1})	Recovery (%)	RSD ($n = 3$, %)
Plasma	0.02	0.021	103.85	0.489
	0.05	0.049	97.38	3.321
	0.1	0.096	95.53	2.152
	0.5	0.493	98.64	2.93
River water	0.02	0.021	104.81	0.572
	0.05	0.048	95.77	3.903
	0.1	0.102	102.03	1.437
	0.5	0.513	102.57	0.880
Tap water	0.02	0.021	104.95	3.31
	0.05	0.050	99.24	2.907
	0.1	0.097	96.86	1.073
	0.5	0.506	101.26	3.784

between 95.77 and 104.81%, with RSD% ≤ 3.903%, indicating the applicability of the method for environmental monitoring. Besides, the analysis of spiked tap water samples showed recovery rates between 96.86 and 104.95% with RSD% ≤ 3.784%, further confirming the reliability of the method for determining lurasidone in different water sources.

3.6. Greenness and blueness assessment

The greenness and blueness of the proposed MPA-CdTe QDs-based fluorescence quenching method were evaluated using the AGREE and BAGI tools, respectively, and compared with previously reported analytical methods for the determination of lurasidone (Fig. 5).

The AGREE tool provides an objective evaluation of the method's environmental impact by evaluating the 12 principles of green analytical chemistry across 12 separate segments in a clock-shaped graph.[31] Each segment corresponds to a specific principle and is color-coded (red, yellow, or green) based on the degree to which the analytical process adheres to green principles. The overall assessment value, ranging from 0 to 1, is depicted in the center of the AGREE graph, with higher values indicating greener analytical procedures. The AGREE score for the proposed method was 0.73, indicating a relatively green analytical process with minimal environmental impact (Fig. 5A). When compared to a previously reported LC-MS method[22] (AGREE score of 0.66), the proposed method demonstrates superior greenness, reflecting the use of less hazardous reagents, reduced energy consumption, and lower waste generation (Fig. 5B). The developed method also outperformed the reported HPLC method[21] in terms of greenness with an AGREE score of 0.73 compared to 0.55 for the HPLC method (Fig. 5C). The factors contributing to the high greenness score include the use of aqueous-based MPA-CdTe QDs as the sensing probe, the optimization of operational parameters to minimize reagent and solvent consumption, and the inherent eco-friendly nature of the fluorescence-based technique. Furthermore, the simple sample preparation, short analysis time, and reduced waste generation also contribute to

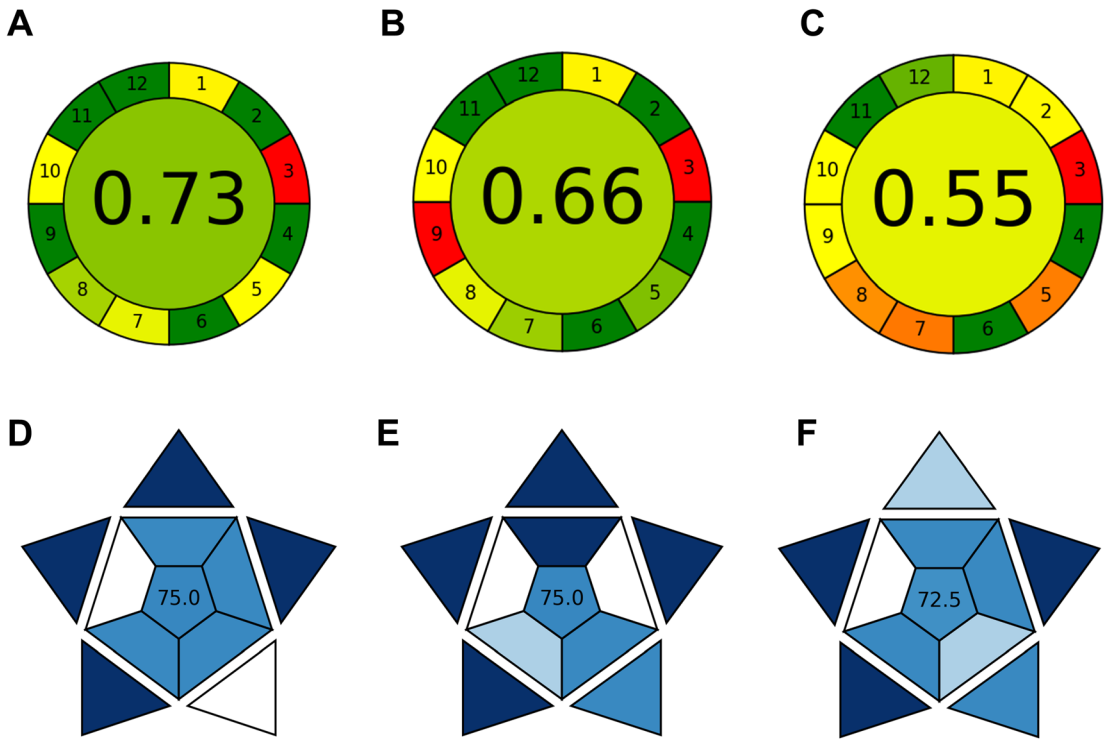

Fig. 5 Greenness and analytical practicality assessment of different methods for lurasidone determination. (A–C) AGREE scores depicting greenness evaluation: (A) proposed MPA-CdTe QDs fluorescence method (0.73), (B) LC-MS method (0.66), and (C) HPLC method (0.55). (D–F) BAGI scores showing analytical practicality: (D) proposed fluorescence method (75.0), (E) LC-MS method (75.0), and (F) HPLC method (72.5).

the overall greenness of the proposed method. However, the use of cadmium-based QDs may raise concerns regarding their potential toxicity, which should be considered in the overall assessment. Besides, the manual handling of the samples unlike automated techniques can also contribute to a lower greenness score.

The analytical practicality of the proposed method was evaluated using the BAGI tool, which considers factors such as simplicity, speed, cost-effectiveness, and ease of use. This tool presents a novel metric for evaluating the practicality of an analytical method by assessing ten critical attributes: type of analysis, simultaneous determination of analytes, sample analysis rate, reagents and materials utilized, necessary instrumentation, level of automation, sample preparation method, simultaneous sample treatment, preconcentration needs, and sample quantity.[32] The BAGI score for the developed method was 75, indicating a highly practical analytical approach (Fig. 5D). Compared to the previously reported LC-MS and HPLC methods, the proposed fluorescence quenching method exhibits similar analytical practicality, with scores of 75 (Fig. 5E) and 72.5 (Fig. 5F), for the LC-MS and HPLC methods respectively. The main advantages of the proposed method include the simplicity of the analytical procedure, the short analysis time, the use of low-cost and widely available instrumentation, and the ease of sample preparation, all of which contribute to its high analytical practicality. The LC-MS and HPLC methods, while providing excellent automation and analytical performance which contributes to their high BAGI scores, they generally require more complex sample preparation, longer analysis times, and more expensive instrumentation, which may limit their applicability in resource-constrained settings.

In summary, the developed MPA-CdTe QDs-based fluorescence quenching method for the determination of lurasidone demonstrates excellent analytical performance, high selectivity, and good accuracy and precision, as well as superior greenness and analytical practicality compared to previously reported methods.

3.7. Comparison with reported literature

The analytical performance of the developed MPA-CdTe QDs-based fluorescence quenching method for lurasidone determination was compared with previously reported methods in the literature. Table 4 summarizes the key analytical parameters of various methods, including chromatographic techniques and sensor-based approaches. The proposed MPA-CdTe QDs-based method offers several advantages over previously reported techniques. While LC-MS/MS methods[22–25] demonstrate better sensitivity with LOQ values as low as 0.25 ng mL^{-1}, these techniques require expensive instrumentation, complex sample preparation, and trained personnel. In contrast, the developed method provides reasonable sensitivity (LOD = 5.90 ng mL^{-1}, LOQ = 17.70 ng mL^{-1}) using simpler instrumentation and less complex analytical procedures. Compared to the conventional HPLC methods,[20,21] the developed approach offers significantly improved sensitivity. The chiral HPLC method reported by Babaker *et al.* has an LOD (0.23 μg mL^{-1}) approximately 39 times higher than the developed method.[21] Furthermore, the linear range of the developed method (0.02–1.0 μg mL^{-1}) is more suitable for trace analysis compared to the broader range (160–1200 μg mL^{-1}) of the HPLC method described by Vaja *et al.*[20]

Interestingly, the developed method shows comparable performance to the recently reported spectrofluorimetric

Table 4 Comparison of the proposed method with previously reported methods for lurasidone determination

Analytical method	Detection system/ nanomaterial	Linear range	LOD	LOQ	Sample matrix	Reference
Fluorescence quenching	MPA-CdTe QDs	0.02–1.0 μg mL^{-1} (20–1000 ng mL^{-1})	5.90 ng mL^{-1}	17.70 ng mL^{-1}	Pharmaceutical formulations, spiked plasma, environmental water	Present work
HPLC-UV	ODS C18 column, UV detection at 230 nm	160–1200 μg mL^{-1}	59.90 μg mL	181.51 μg mL	Pharmaceutical formulations	Vaja *et al.*[20]
HPLC-UV	Chiralcel OD-H column, UV detection at 215 nm	0.78–4.5 μg mL^{-1}	0.23 μg mL^{-1}	0.78 μg mL^{-1}	Pharmaceutical formulations	Babaker *et al.*[21]
LC-MS	Gemini C6-Phenyl column, selected ion monitoring	0.005–5.0 μg mL^{-1} (5–5000 ng mL^{-1})	—	5.0 ng mL^{-1}	Rat plasma, bile, and urine	Chae *et al.*[22]
LC-MS/MS	C18 column, Tandem mass spectrometry	0.25–100 ng mL^{-1} (0.00025–0.1 μg mL^{-1})	—	0.25 ng mL^{-1}	Human plasma	Katteboina *et al.*[23]
LC-MS/MS	C18 column, Tandem mass spectrometry	(0.005–1.2 μg mL^{-1})	—	5.0 ng mL^{-1}	Rat plasma	Rajadhyaksha and Londhe[24]
LC-MS/MS	ODS C18 column, Tandem mass spectrometry	0.002–1.0 μg mL^{-1} (2–1000 ng mL^{-1})	—	2.0 ng mL^{-1}	Rat plasma	Koo *et al.*[25]
Potentiometric sensor	PVC/MIP/MWCNTs on PANI-coated SPE	0.044–44 μg mL^{-1} (10^{-8}–10^{-4} M)	4.4 ng mL^{-1} (10 nM)	—	Pharmaceutical formulations, spiked urine	El-Beshlawy *et al.*[26]
Spectrofluorimetry	Erythrosine B dye	0.02–0.6 μg mL^{-1} (20–600 ng mL^{-1})	4.5 ng mL^{-1}	13.5 ng mL^{-1}	Pharmaceutical formulations	Elhamdy *et al.*[27]

method by Elhamdy *et al.*,[27] which used erythrosine B dye as a fluorescent marker. While their method achieved slightly better sensitivity (LOD = 4.5 ng mL^{-1} *vs.* our 5.90 ng mL^{-1}), the developed approach offers a broader linear range (up to 1000 ng mL^{-1} compared to 600 ng mL^{-1}) and wider applicability to complex biological and environmental matrices beyond pharmaceutical formulations. The potentiometric sensor developed by El-Beshlawy *et al.*[26] shows excellent sensitivity, with a detection limit of 10 nM (approximately 4.4 ng mL^{-1}). However, the developed fluorescence-based method offers comparable sensitivity with broader applicability to different sample matrices, including environmental water samples. In terms of practical applicability, the developed method demonstrates successful application to pharmaceutical formulations, spiked plasma, and environmental water samples, making it more versatile than many of the reported methods that were validated for specific sample types only. Additionally, the developed method incorporates green analytical chemistry principles, as evaluated by AGREE and BAGI tools, further enhancing its appeal as an environmentally friendly analytical approach.

4. Conclusion

The present study reports the development of a sensitive and selective fluorescence quenching method for the determination of lurasidone using MPA-CdTe quantum dots as a "turn-off" fluorescent probe. The proposed method exhibited excellent analytical performance, with good linearity, sensitivity, accuracy, and precision, meeting the requirements of the ICH guidelines. The quenching mechanism was elucidated through Stern–Volmer analysis and thermodynamic studies, revealing that the interaction between lurasidone and MPA-CdTe QDs was predominantly static in nature and spontaneous and exothermic. The influencing factors on the quenching process, including pH, QDs volume, and incubation time, were optimized using a Box–Behnken experimental design, leading to a highly predictive and reliable model. The developed method was successfully applied to the analysis of lurasidone in pharmaceutical dosage forms, spiked plasma, and environmental water samples, demonstrating its versatility and robustness. The greenness and analytical practicality of the proposed method were evaluated using the AGREE and BAGI tools, respectively. The results showed that the MPA-CdTe QDs-based fluorescence quenching method is a greener and more practical alternative to the previously reported analytical techniques for the determination of lurasidone. The present study highlights the potential of MPA-CdTe QDs as a sensitive and selective fluorescent probe for the determination of lurasidone in various matrices, with good analytical performance and environmental compatibility.

While CdTe QDs demonstrate excellent analytical performance, their potential environmental impact due to cadmium toxicity presents a notable limitation. To address this concern, strict waste management protocols can be implemented, including proper collection and disposal of Cd-containing materials. Future research directions may involve the exploration of other types of quantum dots or nanomaterials as fluorescent probes for the development of more sensitive and selective analytical methods for lurasidone and other pharmaceuticals. Particularly promising alternatives can be found in carbon dots, silicon quantum dots, and metal-free fluorescent nanomaterials, which offer reduced environmental impact while maintaining high analytical performance. The transition to these greener alternatives represents an important direction for future method development. Additionally, real sample analysis in a wider range of matrices, such as biological fluids and complex environmental samples, would further demonstrate the robustness and applicability of the proposed method. The development of surface modification strategies to enhance the stability and reduce the environmental impact of quantum dots can also be considered as a valuable direction for future studies.

Data availability

The authors confirm that the data supporting the findings of this study are available within the article and its ESI.†

Conflicts of interest

There are no conflicts to declare.

Acknowledgements

The authors extend their appreciation to Taif University, Saudi Arabia, for supporting this work through project number (TU-DSPP-2024-154).

References

1 S. M. Ng, M. Koneswaran and R. Narayanaswamy, *RSC Adv.*, 2016, **6**, 21624–21661.
2 N. Ullah, M. Mansha, I. Khan and A. Qurashi, *TrAC, Trends Anal. Chem.*, 2018, **100**, 155–166.
3 K. F. Kayani, O. B. A. Shatery, M. S. Mustafa, A. H. Alshatteri, S. J. Mohammed and S. B. Aziz, *RSC Adv.*, 2024, **14**, 5012–5021.
4 K. F. Kayani and K. M. Omer, *New J. Chem.*, 2022, **46**, 8152–8161.
5 K. F. Kayani and C. N. Abdullah, *J. Fluoresc.*, 2025, **35**(2), 1125–1137.
6 S. Sadiq, S. Khan, I. Khan, A. Khan, M. Humayun, P. Wu, M. Usman, A. Khan, A. F. Alanazi and M. Bououdina, *Heliyon*, 2024, **10**, e36189.
7 G. Paramasivam, V. V. Palem, S. Meenakshy, L. K. Suresh, M. Gangopadhyay, S. Antherjanam and A. K. Sundramoorthy, *Colloids Surf., B*, 2024, 114032.
8 J. Wang, D. Li, Y. Qiu, X. Liu, X. Zhang, L. Huang, H. Wen and J. Hu, *Sens. Actuators, B*, 2019, **301**, 126984.
9 J. Jiménez-López, S. S. M. Rodrigues, D. S. M. Ribeiro, P. Ortega-Barrales, A. Ruiz-Medina and J. L. M. Santos, *Spectrochim. Acta, Part A*, 2019, **212**, 246–254.
10 F. Zhang, M. Chen, H. Zhang, H. Xiong, W. Wen, X. Zhang and S. Wang, *Anal. Methods*, 2017, **9**, 929–936.

11 S. S. M. Rodrigues, D. S. M. Ribeiro, L. Molina-Garcia, A. Ruiz Medina, J. A. V. Prior and J. L. M. Santos, *Talanta*, 2014, **122**, 157–165.
12 N. Liang, X. Hu, W. Li, Y. Wang, Z. Guo, X. Huang, Z. Li, X. Zhang, J. Zhang, J. Xiao, X. Zou and J. Shi, *Food Chem.*, 2022, **378**, 132076.
13 J. Jimenez-López, L. Molina-García, S. S. M. Rodrigues, J. L. M. Santos, P. Ortega-Barrales and A. Ruiz-Medina, *J. Lumin.*, 2016, **175**, 158–164.
14 M. Ding, K. Wang, M. Fang, W. Zhu, L. Du and C. Li, *Spectrochim. Acta, Part A*, 2020, **234**, 118249.
15 W. M. Greenberg and L. Citrome, *Clin. Pharmacokinet.*, 2017, **56**, 493–503.
16 J. M. Meyer, A. D. Loebel and E. Schweizer, *Expert Opin. Invest. Drugs*, 2009, **18**, 1715–1726.
17 O. Ichikawa, K. Okazaki, H. Nakahira, M. Maruyama, R. Nagata, K. Tokuda, T. Horisawa and K. Yamazaki, *Neurochem. Int.*, 2012, **61**, 1133–1143.
18 C. Cavallotto, S. Chiappini, A. Mosca, G. d'Andrea, F. Di Carlo, T. Piro, O. Susini, G. Stefanelli, A. Di Cesare, V. Ricci, M. Pepe, L. Dattoli, M. Di Nicola, M. Pettorruso and G. Martinotti, *J. Clin. Med.*, 2024, **13**, 2206.
19 M. Kato, T. Masuda, F. Sano and T. Kato, *J. Affective Disord.*, 2023, **337**, 150–158.
20 M. D. Vaja, R. R. Patel, B. D. Patel and A. B. Chaudhary, *Res. J. Pharm. Technol.*, 2022, **15**, 4999–5004.
21 M. A. Babaker, A. M. Algohary and A. M. Ibrahim, *Sustainable Chem. Pharm.*, 2024, **42**, 101788.
22 Y.-J. Chae, T.-S. Koo and K.-R. Lee, *Chromatographia*, 2012, **75**, 1117–1128.
23 M. Y. Katteboina, N. R. Pilli, R. Mullangi, R. R. Seelam and S. R. Satla, *Biomed. Chromatogr.*, 2016, **30**, 1065–1074.
24 M. Rajadhyaksha and V. Londhe, *Biomed. Chromatogr.*, 2024, **38**, e5764.
25 T.-S. Koo, S.-J. Kim, J. Lee, D.-J. Ha, M. Baek and H. Moon, *Biomed. Chromatogr.*, 2011, **25**, 1389–1394.
26 M. M. El-Beshlawy, A. Barhoum and F. M. Abdel-Haleem, *RSC Adv.*, 2024, **14**, 39769–39778.
27 H. A. Elhamdy, M. Oraby, S. M. Derayea and K. M. Badr El-Din, *Luminescence*, 2024, **39**, e4845.
28 J. Mondal, R. Lamba, Y. Yukta, R. Yadav, R. Kumar, B. Pani and B. Singh, *J. Mater. Chem. C*, 2024, **12**, 10330–10389.
29 F. Pena-Pereira, W. Wojnowski and M. Tobiszewski, *Anal. Chem.*, 2020, **92**, 10076–10082.
30 N. Manousi, W. Wojnowski, J. Płotka-Wasylka and V. Samanidou, *Green Chem.*, 2023, **25**, 7598–7604.
31 K. F. Kayani, S. J. Mohammed, N. N. Mohammad, G. H. Abdullah, D. A. Kader and N. S. Hamad Mustafa, *Food Control*, 2024, **164**, 110611.
32 K. F. Kayani and A. M. Abdullah, *J. Food Compos. Anal.*, 2024, **135**, 106577.